Carbohydrate Polymers 107 (2014) 57–64

Contents lists available at ScienceDirect

Carbohydrate Polymers

journal homepage: www.elsevier.com/locate/carbpol

The preparation, characterization and evaluation of regenerated cellulose/collagen composite hydrogel films

Yongmei Cheng[a,1], Jinting Lu[a,1], Shilin Liu[b], Peng Zhao[c], Guozhong Lu[c], Jinghua Chen[a,*]

[a] School of Pharmaceutical Science, Jiangnan University, Wuxi 214122, China
[b] College of Food Science & Technology, Huazhong Agricultural University, Wuhan 430070, China
[c] The Third Affiliated Hospital of Nantong University, Wuxi 214041, China

ARTICLE INFO

Article history:
Received 5 November 2013
Received in revised form 5 February 2014
Accepted 11 February 2014
Available online 20 February 2014

Keywords:
Cellulose
Film
Collagen
Scaffolds

ABSTRACT

Porous structured regenerated cellulose films were oxidized by periodate oxidation to obtain 2,3-dialdehyde cellulose (DARC) films, which were then reacted with collagen to obtain DARC/Col composite films. The subsequent FT-IR spectra indicated that collagen was immobilized on the DARC matrix via the Schiff base reaction between $-NH_2$ in collagen and $-CHO$ in DARC backbone. Scanning electron microscopy revealed that DARC/Col exhibited a refined 3D network structure and its porosity and pore size decreased with increasing of collagen concentration. The composite films demonstrated a good equilibrium-swelling ratio, air permeability and water retention properties. The composite films also showed excellent mechanical properties, which was vital for practical application. Finally, the cytotoxicity of the composite film was evaluated using NIH3T3 mice fibroblast cells, the results revealed that DARC/Col composite films have good biocompatibility for use as scaffold material in tissue engineering.

1. Introduction

Recent advancements in tissue engineering have led to increased focus on the design and preparation of suitable polymer scaffolds capable of mimicking natural tissue (Palsson & Bhatia, 2004). In natural tissue, extracellular matrix (ECM) components, such as collagen, hyaluronic acid (HA) and fibronectin (FN), are important regulators for cellular growth, proliferation and differentiation in addition to key contributors in the tissue repair and regeneration processes (Adams & Watt, 1993; Clark, 1993). Polymeric scaffolds based on ECM components could replace corrupted or failing ECM in tissue to effectively promote rapid tissue healing and regeneration (Mostow et al., 2005; Vazquez et al., 2003). Collagen, as one of the major components of ECM, exhibits many attractive properties, including low immunogenicity, excellent biocompatibility and biodegradability, enhanced tissue regeneration, and promoted cellular adhesion, growth and proliferation (Lee, Singla, & Lee, 2001; Maeda et al., 1999; Seal, Otero, & Panitch, 2001). It is thus a strong candidate for use in tissue engineering scaffolds. However, when compared with ideal tissue scaffolds, collagen scaffold lacks mechanical properties and shows rapid degradation *in vivo* (Gleeson & O'Brien, 2011). In addressing these issues, extensive research has focused on mixtures of collagen with other biological materials for a composite with improved mechanical properties and stability. For examples, Salome Machado, Martins, and Plepis (2002) and Lu, Feng, Hu, et al. (2008) prepared collagen–chitosan and Collagen–fibroin composite scaffolds via blending and crosslinking; whereas Fischer et al. (2012) prepared collagen/hyaluronic acid porous network scaffold via electrospinning.

Cellulose is a large, linear-chain polymer with an abundance of hydroxyl groups, good biocompatibility and unique physicochemical properties, such as high crystallinity, high water-retention capacity, use of an ultrafine nano-fiber network, high tensile resistance and elasticity modulus. In addition, the fiber structure of cellulose hydrogel is similar to the collagenous fibers found in natural tissue. Cellulose hydrogel is thus considered a promising candidate for collagen-mimicking (Bäckdahl et al., 2008) and for application as a substrate in tissue engineering (Tan, Hong, & Shao, 2007). For tissue repair and regeneration, cellulose has high mechanical strength and good permeability for liquids, gases and electrolytes in a humid environment. It is effective in preventing the accumulation of bacteria and thus avoiding the infection of injured tissue (Gu, Xu, & Hou, 2005). However, cellulose is a polysaccharide and has lower bioactivity and chemical activity compared with proteins such as collagen that show effective cellular growth and proliferation as a result of cell surface receptors.

* Corresponding author. Tel.: +86 51085911900; fax: +86 51085911900.
E-mail address: jhchenwhut@126.com (J. Chen).
[1] These authors contributed equally to this work.

http://dx.doi.org/10.1016/j.carbpol.2014.02.034
0144-8617/

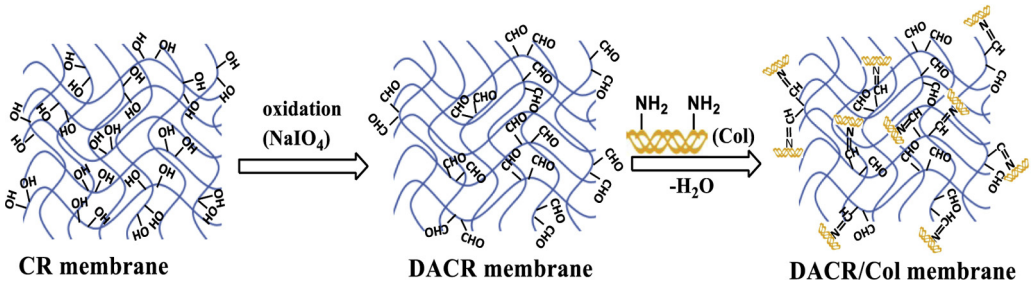

Fig. 1. The schematic diagram of the preparation of DARC/Col composite film.

Therefore, the fixation of proteins or other active factors onto the surfaces of cellulose nano-fibrils could improve the biocompatibility and cytocompatibility of regenerated cellulose film, while preserving the mechanical properties of the scaffold materials (Lin et al., 2011). It is desirable to utilize a scaffold material that has the porosity necessary to support cell in growth and effective mass transport while also supplementing the mechanical properties of engineered tissue (Svenssona et al., 2005). Recently, many studies concerning cellulose/collagen composite materials were documented. They prepared cellulose/collagen composite film either by physical absorption method (Cai & Yang, 2011) or blending and crosslinking method (Li, Guo, & Lan, 2013; Steele, Huang, & Nguyen, 2013). However, physical absorption method can only immobilize tiny amount of collagen and lacks of stability; while blending and crosslinking method may destroy the triple helical conformation and degrade collagen chain, thus lose its bioactivity. Moreover, blending and crosslinking usually needs chemical crosslinking agents, such as glutaraldehyde, which are cytotoxic, and not suitable for *in vivo* application. In our current study, collagen was immobilized on cellulose film without conformation change and degradation, and no crosslinking agent was used. The effectiveness of periodate oxidized regenerated cellulose films for the stabilization of collagen was explored via the Schiff base reaction between —NH_2 in collagen and —CHO in DARC backbone (see Fig. 1). The composite material showed great potential for use as a tissue engineering scaffold due to its high strength in wet state, malleability in situ, good equilibrium-swelling ratio, air permeability and biocompatibility. To the best of our knowledge, this is the first report of self-crosslinked regenerated cellulose–collagen biocomposites as scaffolds for tissue regeneration. The effects of periodates oxidization on regenerated cellulose films were examined in relation to the amount of collagen fixation, swelling behavior, moisture-penetrability and water-retention abilities. The composite materials were also examined for their mechanical properties, microstructure and cell–material interactions to evaluate the potential of the matrix as a scaffold for tissue engineering application.

2. Experimental

2.1. Materials

Native cellulose (the cotton linter pulp) with a viscosity-average molecular weight (M_η) of 1.07×10^5 in cadoxen at 25 °C was supplied by Hubei Chemical Fiber Co. Ltd. (Xiangyang, China). Type I Collagen from bovine tendon with a molecular weight of 298 kDa was supplied by Wuxi Beidi Biological engineering Co. Ltd. (Wuxi, China). Other chemical reagents of analytical grade were supplied by the Sinopharm Chemical Reagent Co. Ltd. (Shanghai, China) and used without further purification.

2.2. Preparation of regenerated cellulose (RC) hydrogel films

The freezing–thawing method was used for dissolving cellulose (Zhang, Ruan, & Gao, 2002). Briefly, native cellulose was dispersed into an aqueous lithium hydroxide/urea solution (4.6 wt%/15.0 wt%) and then placed in a freezer. After freezing, the solution was taken out and thawed at room temperature to obtain a transparent cellulose solution (5 wt%). The obtained cellulose solution was subjected to centrifugation at 7500 rpm and 15 °C for 10 min to eliminate the bubbles in the viscous solution. The bubble-free solution was then cast on a glass plate. The thickness of the solution was controlled at about 1 mm. It was then immersed into a coagulation bath containing 80 vol% ethanol where it coagulated and regenerated for 10 min. The RC hydrogel films were then washed and kept in deionized water until use.

2.3. Preparation of DARC and DARC/collagen hydrogel films

Cellulose hydrogel films were immersed into a 200 mL sodium periodate solution (3%, w/v, 0.14 mol/L) and kept at 37 °C for various time intervals under dark conditions. After the reaction, excess IO_4^- was removed using ethylene glycol and repeated rinsing with distilled water. The yielded wet DARC hydrogel films (oxidized for 2 h) were then reacted with collagen for 24 h at room temperature to prepare DARC/Col hydrogel films. After the reaction, the samples were washed multiple times with distilled water to remove excess collagen. DARC and DARC/Col hydrogel films were then obtained through a freeze drying process.

2.4. Dialdehyde content of DARC hydrogel films

The dialdehyde content of each sample was determined by the Schiff base reaction between aldehyde groups and hydroxylamine hydrochloride (Rosenau et al., 2001). The dialdehyde content (DC) of each sample was calculated through Eq. (1) by Meng, Feng, Liang, et al. (2005).

$$\mathrm{DC}(\%) = \frac{161(V_2 - V_1)}{C_{(\mathrm{HCl})} \times 10^{-3}} \times 100 \quad (1)$$

where V_1 is the amount of hydrochloric acid for titration in mL, V_2 is the amount of hydrochloric acid for control titration in mL, $C_{(\mathrm{HCl})}$ is the concentration of hydrochloric acid in mol/L, m is the weight of each sample, 161 is the average molecular weight when glucose units were translated into 50% dialdehyde.

2.5. Characterization of DARC and DARC/collagen hydrogel films

Fourier-transform infrared spectroscopies (FT-IR) of the samples were recorded with FT-IR spectroscopy (FT-IR 615, Japan). The samples were ground into powders, mixed with KBr and pressed to form a sample disk for FT-IR measurement.

The surface area and the pore structure information (BET and BJH analyses) were obtained using a Micrometrics ASAP 2000 nitrogen adsorption system. BET analysis was carried out for a relative vapor pressure of 0.05–0.3 at 77 K. BJH analysis was performed from the desorption branch of the isotherms.

Scanning electron microscopy (SEM) tests were performed using a Hitachi S4800 (Japan) microscope.

Mechanical properties' testing was performed using a universal tensile tester (CMT 6503, Shenzhen SANS Test Machine Co. Ltd., China) according to ASTM/D638-91 with a speed of 1 mm min^{-1} at room temperature.

2.6. Equilibrium-swelling ratio (Q)

The swelling behavior of the lyophilized films was carried out at pH 7.4 (0.05 M phosphate buffer) at 37 °C. Briefly, the lyophilized film was transferred into a vial containing 15 mL 0.2 M phosphate buffer (pH 7.4) already equilibrated at 37 °C in a shaking water bath. Changes in weight were monitored at time intervals until equilibrium swelling was reached. The equilibrium-swelling ratio (Q) of each sample at time t was obtained as shown in Eq. (2).

$$Q = \frac{W_t - W_0}{W_0} \tag{2}$$

where W_t is the weight of the swollen sample at time t and W_0 is the weight of the lyophilized sample. Five replicates were performed to obtain an average value of Q.

2.7. Water vapor transmission rate (WVTR) and water retention (WR)

The water vapor transmission rate (WVTR) of the film specimens was measured according to the modified ASTM E96 method (ASTM, 2000; Ou, Kwok, & Kang, 2004). Glass cups with a diameter of 3 cm and depth of 4 cm were used. To maintain 0% RH in the cup headspace, 3 g of dried $CaCl_2$ was added to the cup. The film was then sealed over the rim of the cup with the application of molten paraffin. The cups were placed in hermetically sealed jars and maintained at 37 °C and 75% RH (using saturated NaCl solution). 1000 mL of water was placed in the bottom of the jar to maintain the RH. The cups were then weighed every 1 h for 3 days. The amount of water that permeated through the films was determined from the weight gain of the cups. WVTR and water vapor permeability (WVP) were calculated as shown in Eq. (3) (Toméa et al., 2011).

$$\mathrm{WVTR} = \frac{\Delta w}{\Delta t} \cdot A$$
$$\mathrm{WVP} = \frac{\mathrm{WVTR} \cdot L}{\Delta p} \tag{3}$$

where WVTR is in g/s m^2, $\Delta w/\Delta t$ is the rate of water gain in s/h, A is the exposed area of the film in m^2, L is the mean thickness of samples in m and Δp is the difference in partial water vapor pressure between the two sides of film samples in Pa. The water vapor pressure on the high-stream side of the film was 3.2 kPa (water vapor pressure of saturated NaCl aqueous solution at 37 °C), while the low-stream side was assumed to be zero.

The water retention levels of the wet samples were examined using a desiccator (with a relative humidity of 79%) at 37 °C. The wet samples were weighed and then placed in the aforementioned desiccator. Then, the samples were taken out and weighed at various time intervals. The weight remaining (WR) ratio of each sample at time t was calculated as the ratio of the weight at time t (W_t) to the initial weight (W_0) as shown in Eq. (4).

$$\mathrm{WR}(\%) = \frac{W_t}{W_0} \times 100 \tag{4}$$

where W_0 is the initial weight and W_t is the weight at time t.

2.8. Biocompatibility assessments

2.8.1. Cell culture

The NIH3T3 cells (provided by the Cell Bank, Chinese Academy of Sciences, Shanghai, China) were cultured in DMEM medium (Gibco, USA) with penicillin (100 IU/mL), streptomycin (100 IU/mL) and amphotericin b (100 IU/mL) supplemented with 10% fetal bovine serum (Gibco, USA) at 37 °C in a 5% CO_2 humidified incubator (Thermo, USA). The culture medium was changed every two days and cells were passaged in logarithmic growth phase.

All of the samples were sterilized by Co^{60} prior to the cell culture experiments. The sterilized samples were then placed in a 24-well tissue culture plate with the addition of 1 mL DMEM complete medium. After 4 h, the medium was removed and replaced by 1 mL NIH3T3 cell suspension. The density of the NIH3T3 cell utilized for seeding was 3×10^4 cells/mL.

2.8.2. MTT assay

The growth and proliferation of the NIH3T3 cells on the surface of the scaffolds were evaluated by MTT assay after 1, 3 and 5 days of culturing, respectively. All of the samples were then harvested and washed by sterilized PBS (pH 7.4) to remove non-adherent cells and then transferred to a new tissue culture plate. Subsequently, 550 μL sterilized PBS (pH 7.4) containing 5 mg/mL MTT reagent (Sigma, USA) was added and incubated at 37 °C for 4 h. The culture medium was removed and the samples were washed thrice with PBS. Then, 100 μL of dimethyl sulfoxide (DMSO, 500 μL/well, Sigma, USA) was added, and the cells were shaken for 10 min under 37 °C. The optical densities at 570 nm were measured by an ELISA microplate reader (Thermo, USA).

2.8.3. Morphology of NIH3T3

To study the morphology of the NIH3T3 cellular attachment and growth on the samples, we performed fluorescence staining of cells using fluorescein diacetate (FDA, Sigma, USA) and observed them under fluorescence inverted microscope (Leica, DMIL LED Fluo, Germany). NIH3T3 cells were seeded onto the samples with the density of 2×10^4 cells/mL and incubated at 37 °C for 4 h, 1, 3, and 5 days under the same culture mentioned above, respectively. Afterward, all of the samples were then harvested and washed by sterilized PBS (pH 7.4) to remove non-adherent cells and then transferred to a new tissue culture plate. Then 0.05 mg/mL FDA dye in sterilized PBS (pH 7.4, 500 μL) was added and incubated 20 min at 37 °C. The culture medium was removed and the samples were washed thrice with PBS. Finally, the samples were kept in dark place and photographed using a fluorescence inverted microscopy.

2.9. Statistical analysis

All of the experimental data were collected in triplicate and the values were expressed as the mean ± standard deviation (SD). Statistical distinctions were analyzed by Student's paired t-test and the statistical significance was determined in relation to the probability (P) values $P < 0.05$.

3. Results and discussion

3.1. The dialdehyde content of DARC hydrogel films

Periodate is known to oxidize the vicinal hydroxyl groups of cellulose at positions 2 and 3 to aldehyde groups, simultaneously breaking the corresponding carbon–carbon bond of the glucopyranose ring in order to obtain 2,3-dialdehyde cellulose (DAC). The

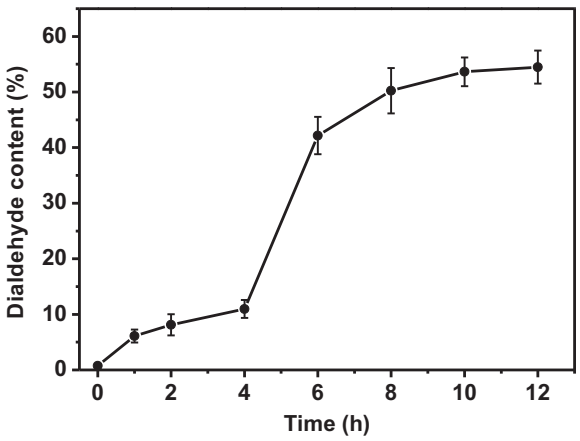

Fig. 2. Dialdehyde content curve of DARC (oxidation with $NaIO_4$) related to reaction time.

aldehyde groups of DAC have high reactivity toward further modification such as to react with the amino group of collagen via Schiff base reaction. Fig. 2 shows the dialdehyde content of different DARC films. With increasing of reaction time, the dialdehyde degree of the oxidized cellulose increased from 0.73% to 54.49%, while the reaction rate low within the first 4 h but too much higher at time point of 6 h. Because regenerated cellulose film contains amorphous region and crystal region. The crystal regions are very tight structure and hard to be oxidized at the beginning of the oxidation reaction. It should be noted that too high dialdehyde degree in the oxidized cellulose matrix may result in poor mechanical properties due to side reactions, such as peeling reactions (Yang, 2006). So we chose DARC with oxidizing for 2 h for the next preparation of DARC/Col composite film.

3.2. The characterization of DARC and DARC/collagen hydrogel films

Fig. 3 shows the SEM images of the freeze-dried RC, DARC and DARC/Col composite hydrogel films. The RC hydrogel films presented a porous structure, composing of fibrils with diameter about 20 nm. These fibrils were tangled with each other and formed

Table 1
The S_{BET}, V_{BJH} and D_{BJH} of RC, DARC, and DARC/Col membranes.

Sample	S_{BET} (m^2/g)[a]	D_{BJH} (nm)[b]	V_{BJH} (cm^3/g)[c]
RC	90.78	11.47	0.770
DARC/Col	2.08	9.07	0.023

[a] Data obtained from BET with a relative vapor pressure of 0.05–0.3 of desorption branch.
[b] Data from BJH desorption branch.
[c] Data from BJH desorption branch.

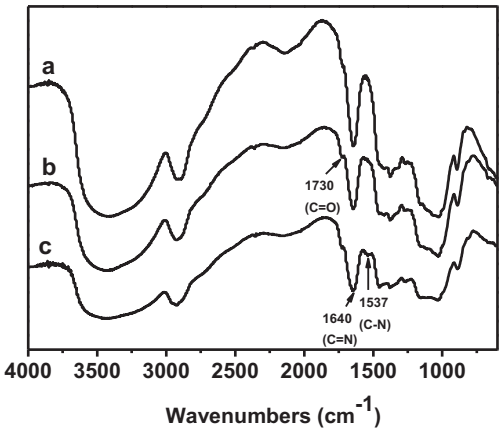

Fig. 4. FT-IR spectra of (a) RC, (b) DARC (oxidized for 2 h) and (c) DARC/Col (react with 5 mg/mL Col solution) films.

interconnected networks. This unique structure was ascribed to the phase separation of the cellulose solution during the regeneration process, where solvent-rich regions contributed to the formation of pores. The 3D network structure was still preserved in DARC following the oxidation of RC hydrogel films by $NaIO_4$ (Fig. 3b). One distinct change in morphology after periodate oxidation was the RC pellicles shrank obviously and the diameter of the fiber in nanonetwork increased (Fig. 3b). After the immobilization of collagen, the composite hydrogel films showed a different morphology to that of RC or DARC films. When DARC film reacted with collagen at lower concentrations, thin collagen coatings formed and enwrapped onto the surfaces of the DARC nanofibers leading to

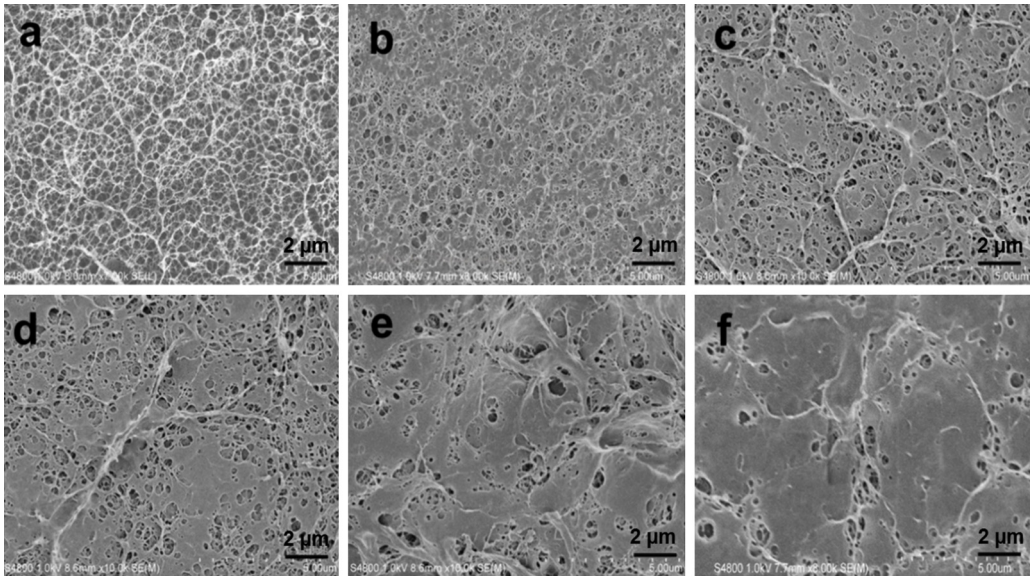

Fig. 3. SEM micrographs of (a) RC, (b) DARC (oxidized for 2 h), (c) DARC/Col (react with 1 mg/mL Col solution), (d) DARC/Col (react with 2 mg/mL Col solution), (e) DARC/Col (react with 4 mg/mL Col solution) and (f) DARC/Col (react with 5 mg/mL Col solution) films, scale bar: 2 μm.

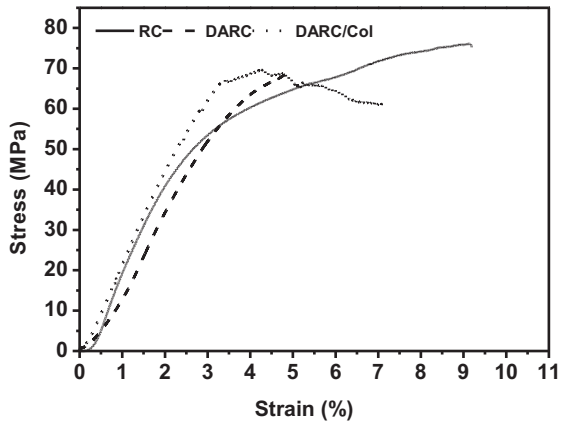

Fig. 5. Stress–strain curves of dry RC, DARC (oxidized for 2 h) and DARC/Col (react with 5 mg/mL Col solution) films.

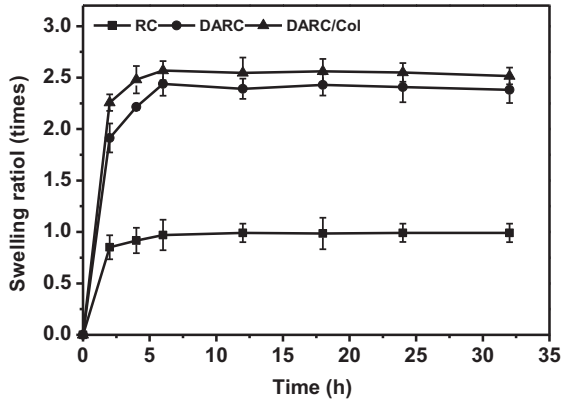

Fig. 6. Swelling behavior of RC, DARC (2 h oxidation with $NaIO_4$) and DARC/Col (react with 5 mg/mL Col solutions) films.

the preservation of the 3-D network (Fig. 3c and d). In contrast, when DARC film treated with collagen at higher concentrations, the surface of the DARC film was almost completely covered by collagen (Fig. 3e and f). Nevertheless, all of these results indicated that collagen was immobilized onto the DARC hydrogel films. So we chose DARC/Col with immobilizing 5 mg/mL collagen for the ultima DARC/Col composite film.

The S_{BET}, V_{BJH} and D_{BJH} data of the freeze-dried RC and DARC/Col films were summarized in Table 1. The BET surface area (S_{BET}) of RC and DARC/Col films are 90.78 m^2/g and 2.08 m^2/g, respectively,

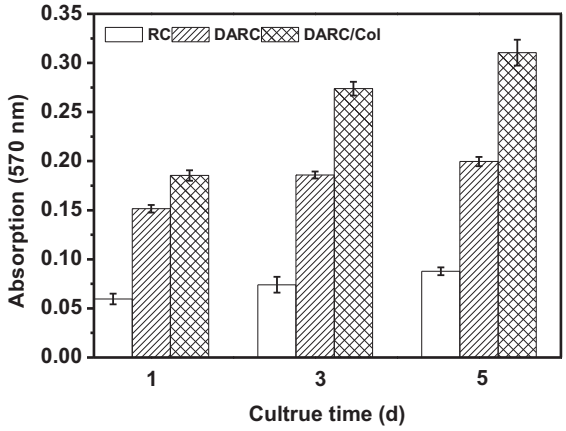

Fig. 8. MTT assay for growth and proliferation of cells cultured on the RC, DARC (oxidized for 2 h), and DARC/Col (react with 5 mg/mL Col solutions) films after incubation for various periods.

indicating both films were porous structure. In general, the higher S_{BET} value implies a more porous structure. Thus, immobilization of collagen decreased surface area of RC films. The V_{BJH} and D_{BJH} data of DARC/Col film were 0.023 cm^3/g and 9.07 nm, which were lower than that of RC films (0.770 cm^3/g and 11.47 nm), suggesting the decreasing in both pore volume and pore diameter.

Fig. 4 shows the FT-IR spectra of the RC, DARC and DARC/Col hydrogel films. Oxidized cellulose (DARC) exhibited two characteristic FT-IR bands near 1740 and 880 cm^{-1}, which were attributed to C=O stretching and the formation of hemiacetal bonds between newly achieved aldehyde groups and their neighboring hydroxyl groups (Fig. 4b). There was an intensity variation at 1640 cm^{-1} (–C=N– band) and 1530 cm^{-1} (amide II band) in the FT-IR spectrum of DARC/Col films, which were the characteristic absorption peaks of Col (Fig. 4c). Compared with the spectrum of DARC films, the absorption of C=O and hemiacetal bonds was negligible. These results suggested that Col was immobilized onto the DARC hydrogel films as illustrated in Fig. 3.

Fig. 5 shows the typical stress–strain curves of RC, DARC and DARC/Col films. The stress and strain points at break for RC, DARC and DARC/Col gel films were measured as 73.5 MPa, 9%; 65.63 MPa, 6.09%; and 65.82 MPa, 6.35%; respectively. Clearly, DARC and DARC/Col gel films had lower stress and strain points at break than RC gel films, indicating that the oxidation of $NaIO_4$ led to the destruction of the molecular structure and polymerization degree of RC gel films. It must be noted that the DARC/Col films showed good mechanical properties when compared with

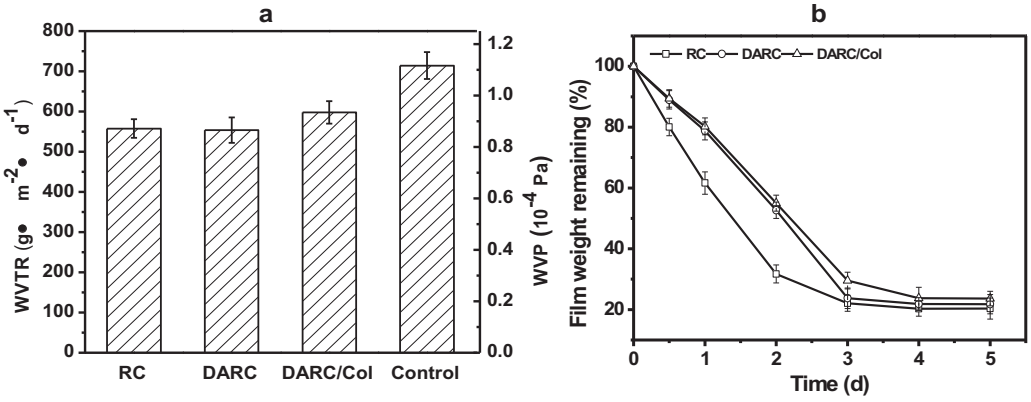

Fig. 7. Properties analysis of samples: (a) WVTR and WVP of RC, DARC (2 h oxidation with $NaIO_4$) and DARC/Col (react with 5 mg/mL Col solutions) membranes and (b) water loss curves of RC, DARC (oxidized for 2 h), and DARC/Col (react with 5 mg/mL Col solutions) films.

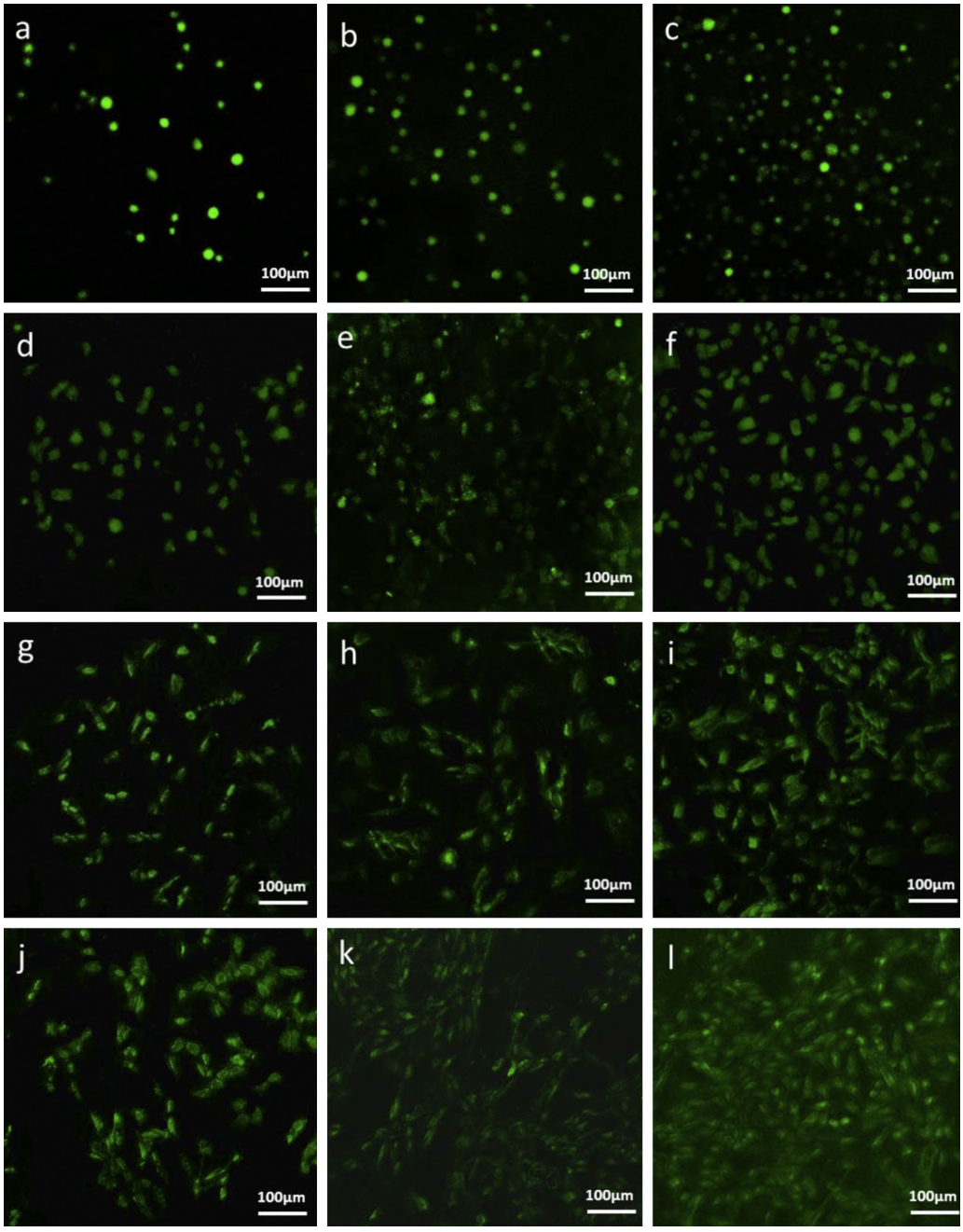

Fig. 9. The attachment and growth of NIH3T3 cells on RC, DARC (oxidized for 2 h), DARC/Col (react with 5 mg/mL Col solutions) films after *in vitro* culture for 4 h (a–c), 1 day (d–f), 3 day (g–i), and 5 day (j–l), respectively.

other recently used similar materials, such as Intrgra®, Pelnac®, Biofill®, and Gengiflex®, whose mechanical strength were 0.48 MPa or lower (Ng, Khor, & Hutmacher, 2004). It was well known that the design and preparation of the seed cell survival polymer scaffold must have a good balance between mechanical strength and porosity. Good mechanical strength is required for tissue regeneration in situ, while porosity is needed for conducive cell growth *in vitro* and *in vivo* (Thomson et al., 1995).

3.3. Equilibrium-swelling ratio (Q)

Swelling behavior in the composite films is vital for practical application in tissue engineering. *In vitro* testing has indicated that rapid swelling behavior in materials assists in cell adhesion and growth (Shanmugasundaram et al., 2001). Fig. 6 shows the swelling degree of the RC, DARC and DARC/Col films at 37 °C in 0.2 M phosphate buffer solution (pH 7.4). The DARC/Col films showed increased solution uptake behavior compared with pure RC or DARC films. The equilibrium swelling ratio of RC, DARC and DARC/Col films were 99%, 230% and 252%, respectively. DARC/Col film had the highest equilibrium ratio, which was more than 2.5 times than that of RC film. This could be attributed to the oxidation of the cellulose matrix and interior structure of RC in addition to the destruction of some of the crystalline regions. Furthermore, the immobilization of Col on the DARC films could also enhance the swelling degree of the DARC/Col films. These results indicated that the RC films modified with Col had an obviously improved swelling ratio, which is vital for the removal of exudates from wounds.

3.4. Water vapor transmission rate (WVTR) and water retention (WR)

Fig. 7a shows the water vapor transmission rate (WVTR) and water vapor permeability (WVP) of RC, DARC and DARC/Col films when placed in a humid environment (with a relative humidity of 75%) at 37 °C. The WVTR and WVP of the RC, DARC and DARC/Col films were 557.68 g m^{-2} d^{-1}, 0.87×10^{-4} Pa; 553.86 g m^{-2} d^{-1}, 0.87×10^{-4} Pa; and 597.57 g m^{-2} d^{-1}, 0.93×10^{-4} Pa; respectively. There were no significant differences in the WVTR of the films. Materials for tissue repair should have a WVTR in the range of 480–720 g m^{-2} d^{-1} for clinical application (Gu & Xu, 1993). Therefore, the WVTR levels suggested that all of the films illustrated potential for use as a tissue repair material.

The water loss of each film in a humid environment (with a relative humidity of 79%) at 37 °C was shown in Fig. 7b. The samples showed rapid water loss in the first three days (about 70%), which reduced over the next 2 days (about 10%). There was no obvious difference among the samples. However, all of the samples still retained approximately 20% of water after exposure to the above conditions for 5 days. These results indicated that the immobilization of Col could prolong the humid microenvironment period on the wound.

3.5. Biocompatibility assessments

Surface cellular growth and proliferation over time are a symbol of cytocompatibility for materials and can be used for assessing the potential of materials for application in tissue engineering. To detect cellular growth and proliferation on the Col-immobilized samples, NIH3T3 mice fibroblast cells were seeded on the surface of each sample. After incubation for 1, 3 and 5 days, the amount of NIH3T3 was measured by MTT assay. Fig. 8 shows the quantity and proliferation of NIH3T3 on the surface of the RC, DARC and DARC/Col films. At the beginning of the culture (1st day), the DARC/Col films surface attached more NIH3T3 compared with that of RC and DARC films, i.e., the cells on DARC/Col film surface were more than 3 times of that on RC film surfaces. NIH3T3 cells on the DARC/Col film surface showed rapid proliferation compared with those on RC and DARC film surfaces. After incubation for 5 days, cells on DARC/Col film surface were approximately 4 times of that on RC film surface. Our results indicated that Col-immobilized on RC films was not only increased NIH3T3 cells adhesion on film surface but also promoted cells growth and proliferation. This may be attributed to the increased swelling degree of DARC/Col film (Shanmugasundaram et al., 2001) as well as the existing of cell-binding domains in collagen structure.

The proliferation and cytoskeleton of NIH3T3 could be detected by FDA fluorescence staining and observed under fluorescence inverted microscope. Fig. 9 showed the density and cytoskeleton of NIH3T3 on different films after incubation for 4 h, 1, 3, and 5 days, respectively. The NIH3T3 cells seeded on films exhibited elliptical, spindle or polygonal morphology. Clearly, more NIH3T3 cells attached to DARC/Col film and they grew fast than the cells on RC and DARC films. On the fifth day, the DARC/Col film surface was almost covered by NIH3T3 cells with elliptical morphology and they trended to aggregate, indicating an obvious cytoskeleton organization and proliferation on the surface of DARC/Col. These results showed that the spreading and proliferation of NIH3T3 cells on the surface of DARC/Col was enhanced.

4. Conclusions

DARC/Col composite films were obtained by immersing DARC wet films into Col aqueous solution and immobilizing Col onto the DARC films via the Schiff base reaction. The surface topography and microstructure revealed that DARC/Col exhibited a refined 3D network structure where porosity and pore size decreased with increasing collagen concentration. Meanwhile, Col-immobilized films demonstrated improved WVTR and WVP, equilibrium-swelling ratio and water retention than RC films. Biocompatibility assessments of the films indicated that Col-immobilized DARC/Col films were the most efficient in promoting cellular growth and proliferation. NIH3T3 cell exhibited elliptical morphology and trend to aggregate on DARC/Col film. The results highlighted the potential of DARC/Col composite films for practical application as a tissue repair material.

Acknowledgements

This work was supported by the National Natural Science Foundation of China (51003043, 81272106, 21306066), the Research Fund for the Doctoral Program of Higher Education of China (20110093110008), and the Natural Science Foundation of Jiangsu Province (BK2011186).

References

Adams, J. C., & Watt, F. M. (1993). Regulation of development and differentiation by the extracellular matrix. *Development*, *117*, 1183–1198.
ASTM Standard E96-00. (2000). *Standard test methods for water vapor transmission of materials. Annual book of ASTM standards* (Vol. 4.06) Philadelphia: ASTM.
Bäckdahl, H., Esguerra, M., Delbro, D., Risberg, B., & Gatenholm, P. (2008). Engineering microporosity in bacterial cellulose scaffolds. *Journal of Tissue Engineering and Regenerative Medicine*, *2*, 320–330.
Cai, Z. J., & Yang, G. (2011). Bacterial cellulose/collagen composite: Characterization and first evaluation of cytocompatibility. *Journal of Applied Polymer Science*, *120*, 2938–2944.
Clark, R. A. (1993). Basics of cutaneous wound repair. *Journal of Dermatologic Surgery and Oncology*, *19*, 693–706.
Fischer, R. L., Mccoy, M. G., & Grant, S. A. (2012). Electrospinning collagen and hyaluronic acid nanofiber meshes. *Journal of Materials Science: Materials in Medicine*, *23*, 1645–1654.
Gu, H. Q., & Xu, G. F. (1993). *Biomedical materials*. Tian Jin: Tianjin Science and Technology Translation Press.
Gu, Q. S., Xu, Z., & Hou, C. L. (2005). *Practice biomedical material*. Shanghai: Shanghai Science and Technology Press.
Gleeson, J. P., & O'Brien, F. J. (2011). Composite scaffolds for orthopaedic regenerative medicine. *Advances in Composite Materials for Medicine and Nanotechnology*, *10*, 33–58.
Lee, C. H., Singla, A., & Lee, Y. (2001). Biomedical applications of college – A review. *International Journal of Pharmaceutics*, *221*, 1–22.
Li, W. C., Guo, R., & Lan, Y. (2013). Preparation and properties of cellulose nanocrystals reinforced collagen composite films. *Journal of Biomedical Materials Research Part A*, http://dx.doi.org/10.1002/jbm.a.34792
Lin, Y. K., Chen, K. H., Ou, K. L., & Liu, M. (2011). Effects of different extracellular matrices and growth factor immobilization on biodegradability and biocompatibility of macroporous bacterial cellulose. *Journal of Bioactive and Compatible Polymers*, *265*, 508–518.
Lu, Q., Feng, Q., Hu, K., & Cui, F. (2008). Preparation of three-dimensional fibroin/collagen scaffolds in various pH conditions. *Journal of Materials Science: Materials in Medicine*, *19*, 629–634.
Maeda, M., Tanis, S., Sano, A., & Fujioka, K. (1999). Microstructure and release characteristics of the minipellet, a college based drug delivery system for controlled release of protein drugs. *Journal of Controlled Release*, *62*, 313–324.
Meng, S., Feng, Y., Liang, Z., Fu, Q., & Zhang, E. (2005). Oxidizing cellulose to 2,3-dialdehyde cellulose by sodium periodate. *Transactions of Tianjin University*, *11*, 250–254.
Mostow, E. N., Haraway, G. D., Dalsing, M., Hodde, J. P., & King, D. (2005). Effectiveness of an extracellular matrix graft (OASIS Wound Matrix) in the treatment of chronic leg ulcers: A randomized clinical trial. *Journal of Vascular Surgery*, *41*, 837–843.
Ng, K. W., Khor, H. L., & Hutmacher, D. W. (2004). In vitro characterization of natural and synthetic dermal matrices cultured with human dermal fibroblasts. *Biomaterials*, *14*, 2807–2818.
Ou, S. Y., Kwok, K. C., & Kang, Y. J. (2004). Changes in vitro digestibility and available lysine of soy protein isolate after formation of film. *Journal of Food Engineering*, *64*, 301–305.
Palsson, B. O., & Bhatia, S. N. (2004). *Tissue engineering*. New Jersey: Pearson Pentice Hall.
Rosenau, T., Potthast, A., Silxta, H., & Kosma, P. (2001). The chemistry of side reactions and byproduct formation in the system NMMO/cellulose (Lyocell process). *Progress in Polymer Science*, *26*, 1763–1837.
Salome Machado, A. A., Martins, V. C. A., & Plepis, A. M. G. (2002). Thermal and rheological behaviour of collagen–chitosan blends. *Journal of Thermal Analysis and Calorimetry*, *67*, 491–498.

Seal, B. L., Otero, T. C., & Panitch, A. (2001). Polymeric biomaterials for tissue and organ regeneration. *Materials Science and Engineering: R: Reports*, *34*, 147–230.

Shanmugasundaram, N., Ravichandran, P., Neelakanta, R. P., Ramamurty, N., Pal, S., & Panduranga, P. K. (2001). Collagen-chitosan polymeric scaffolds for the in vitro culture of human epidermoid carcinoma cells. *Biomaterials*, *22*, 1943–1951.

Steele, T. W. J., Huang, C. L., & Nguyen, E. (2013). Collagen–cellulose composite thin films that mimic soft-tissue and allow stem-cell orientation. *Journal of Materials Science: Materials in Medicine*, *24*, 2013–2027.

Svenssona, A., Nicklassonb, E., Harraha, T., Panilaitis, B., Kaplan, D. L., Brittberg, M., et al. (2005). Bacterial cellulose as a potential scaffold for tissue engineering of cartilage. *Biomaterials*, *26*, 419–431.

Tan, Y. J., Hong, F., & Shao, Z. Y. (2007). Advances in applications of bacterial cellulose in biomedical materials. *China Biotechnology*, *27*, 126–131.

Thomson, R. C., Yaszemski, M. J., Powers, J. M., & Mikos, A. G. (1995). Fabrication of biodegradable polymer scaffolds to engineer trabecular bone. *Journal of Biomaterials Science Polymer Edition*, *7*, 23–38.

Toméa, L. C., Goncalvesa, C. M. B., Boaventurab, M., Brandão, L., Mendes, A. M., Silvestre, A. J. D., et al. (2011). Preparation and evaluation of the barrier properties of cellophane films modified with fatty acids. *Carbohydrate Polymers*, *83*, 836–842.

Vazquez, J. R., Short, B., Findlow, A. H., Nixon, B P, Boulton, A. J., & Armstrong, D. G. (2003). Outcomes of hyaluronan therapy in diabetic foot wounds. *Diabetes Research and Clinical Practice*, *59*, 123–127.

Yang, S. H. (2006). *Plant fiber chemistry*. Beijing: Light Industry Press.

Zhang, L. N., Ruan, D., & Gao, S. (2002). Dissolution and regeneration of cellulose in NaOH/thiourea aqueous solution. *Journal of Polymer Science Part B: Polymer Physics*, *14*, 1521–1529.